Influence of Pressure, Velocity and Fluid Material on Heat Transport in Structured Open-Cell Foam Reactors Investigated Using CFD Simulations

Christoph Sinn [1] **, Jonas Wentrup** [1]**, Jorg Thöming** [1,2] **and Georg R. Pesch** [1,2,*]

[1] Faculty of Production Engineering, Chemical Process Engineering Group, University of Bremen, Leobener Strasse 6, 28359 Bremen, Germany; sinn@uni-bremen.de (C.S.); jwentrup@uni-bremen.de (J.W.); thoeming@uni-bremen.de (J.T.)

[2] MAPEX Center for Materials and Processes, University of Bremen, Postbox 330 440, 28334 Bremen, Germany

[*] Correspondence: gpesch@uni-bremen.de

check for updates

Abstract: Structured open-cell foam reactors are promising for managing highly exothermic reactions such as CO_2 methanation due to their excellent heat transport properties. Especially at low flow rates and under dynamic operation, foam-based reactors can be advantageous over classic fixed-bed reactors. To efficiently design the catalyst carriers, a thorough understanding of heat transport mechanisms is needed. So far, studies on heat transport in foams have mostly focused on the solid phase and used air at atmospheric pressure as fluid phase. With the aid of pore-scale 3d CFD simulations, we analyze the effect of the fluid properties on heat transport under conditions close to the CO_2 methanation reaction for two different foam structures. The exothermicity is mimicked via volumetric uniformly distributed heat sources. We found for foams that are designed to be used as catalyst carriers that the working pressure range and the superficial velocity influence the dominant heat removal mechanism significantly. In contrast, the influence of fluid type and gravity on heat removal is small in the range relevant for heterogeneous catalysis. The findings might help to facilitate the design-process of open-cell foam reactors and to better understand heat transport mechanisms in foams.

Keywords: computational fluid dynamics (CFD); conjugate heat transfer; open-cell foams; structured reactors; volumetric heat sources; fluid properties; STAR-CCM+; dynamic operation

1. Introduction

Open-cell foams are promising monolithic catalyst support structures for exo- and endothermal heterogeneous gas-phase reactions such as the CO_2 methanation, due favorable characteristics such as good heat transport, low pressure drop and high porosities [1–3]. The CO_2 methanation currently attracts much attention in the chemical engineering community as it can be a cornerstone the future transition to a sustainable energy supply within the Power-to-X (PtX) concept [4]. Here, excess energy from wind turbines or solar panels is converted via electrolysis into hydrogen, and usually reacted catalytically with carbon dioxide to methane. As the power grids might not be resilient enough to withstand the high energy load during wind or sun peak hours, dynamically operated small-scale plants for storage of excess energy are needed in the future [5]. Small-scale plants are operated at low flow rates making heat removal traditionally difficult. The dynamic operation can cause tremendous jumps of pressure, velocity and even change the fluid composition resulting in undesired or uncontrollable temperature increases. Thus, the heat transport (and heat removal) inside these reactors needs to be addressed to protect the catalyst's activity and ensure safe as well as robust operation [6]. Generally,

for the methanation reaction, low temperatures are thermodynamically favorable [7]. Therefore, an effective heat removal ensures efficient conversion and protects the catalyst particles from sintering.

Recently it was shown that, at low flowrates, foam-structured reactors can be advantageous over conventional pellets for CO_2 methanation [8]. The reason is that heat is dominantly removed via radial conduction in foam reactors, whereas pellets in fixed-bed reactors remove heat axially via convection [9]. However, only when heat conduction dominates over convection, foams can be advantageous over pellets as pellets generally have a higher axial convective heat transport [8].

To study heat flows and heat transport mechanisms in structured reactors, computational fluid dynamics (CFD) simulations have been well established [10]. With the aid of CFD simulations, the three heat transport mechanisms, conduction [11,12], convection [13,14] and radiation [15], have been addressed in open-cell foams. Among others, the influences of superficial velocity [16,17], wall coupling [18], solid thermal conductivity [19], geometrical influences (i.e., strut shape [20,21] and porosity [22,23]) on heat transport were studied simulatively. Most of the studies targeted solely heat transport in the solid or conjugate heat transport between a fluid and a foam with no superimposed catalytic reaction. Simulations of detailed catalytic reactions on foams are costly and only a few studies have been published so far that mainly dealt with the CO oxidation reaction [24–28].

In order to reduce complexity of the reaction system and to speed up simulations, we recently proposed to mimic exothermal reactions via uniformly distributed heat sources in the solid foam [19]. Heat sources (or heat sinks) mimic the exothermicity (or endothermicity) and can be used to study heat flows and temperature increases in open-cell foams decoupled from reaction mechanisms. This approach has been utilized to study the influence of heat sources intensities (from 5–150 W), laminar superficial velocities (0–0.5 m s^{-1}), solid thermal conductivities (1–200 W m^{-1} K^{-1}), and thermal radiation (temperature levels 500–1200 K, solid emissivities 0–1) [15,19]. It was found that the solid thermal conductivity and the superficial velocity are key parameters for designing efficient heat-removing foams for the usage as catalyst carriers [19]. Moreover, for reactor tube diameters below 25 mm and superficial velocities lower than 0.5 m s^{-1}, the investigated structure (irregular foam) showed conduction being the dominant heat removal mechanism (this parameter range is in relevant order of magnitude for decentralized small scale methanation plants [29,30]). Furthermore, thermal radiation can contribute significantly to the heat transport at conditions relevant for methanation [15].

Our previous studies focused mainly on the properties of the solid foam, whereas the fluid has only been addressed by ramping the superficial velocity in the laminar regime for air at 1 bar pressure [15,19]. Other CFD studies dealing with heat transport in foams also mainly considered air as fluid with often constant fluid properties such as density, thermal conductivity and specific heat [16,22,31,32]. The study of Razza et al. investigated the influence of wall coupling between foam and tubular wall utilizing He as well as N_2 as fluids [18]. They found significant changes in computed fluid temperatures and justified the deviation through the six times higher thermal conductivity of He (they also assumed constant fluid properties). Additionally, Bianchi et al. [31] found a significant difference for computed heat transfer of either air or water (liquid).

The methanation reaction (CO_2 + $4H_2$ $\rightleftarrows$ CH_4 + $2H_2O$), however, involves gas mixtures (CO_2, H_2 and CH_4), higher velocity ranges (i.e., ≥0.5 m s^{-1}) and elevated pressure ranges (4–10 bar) [6]. Furthermore, the effect of gravitational acceleration has not been addressed so far in CFD studies of heat transport in open-cell foams. This might be relevant, because reactors can be operated vertically or horizontally leading to a different effective direction of gravity (i.e., natural convection).

In this study, we thus investigate the influence of the fluid properties on the overall heat transport, heat flows, and solid temperatures; a topic which has largely been neglected in the past. In detail, we analyze the influence of pressure, velocity, fluid composition and gravitational acceleration on the dominant heat transport (i.e., heat removal) mechanisms. We further determine under what circumstances the fluid properties need to be explicitly accounted for to study catalyst carriers for, e.g., the CO_2 methanation reaction.

2. Materials and Methods

The CFD model investigated in this study consists of a foam embedded in a tube (i.e., a tubular structured reactor) and is similar to our previous study [19]. The problem is the steady-state conjugate heat transfer between the flowing fluid and the foam. The simulations were carried out with the commercial CFD software STAR-CCM+ from Siemens PLM (Plano, TX, USA) [33]. Heat production through exothermal reactions is represented by volumetric homogeneously distributed heat sources in the solid (S = 12.5 W in all cases) [19]. The heat source intensity of 12.5 W was chosen as it corresponds to the heat released during the CO_2 methanation for a foam in this order of magnitude (50 W for a full sponge equals 12.5 W for one quarter of the sponge) [19].

Two foams (radius 7.5 mm; length 20 mm) are investigated in this study, modeled through Kelvin cell lattices (KC1 and KC2) that differ strongly in their strut diameter (see Figure 1 and Table 1). Only a quarter of the foams as well as the pipe are simulated due to the regularity of the structure and to further reduce computational cost. Polyhedral meshes were created using the integrated STAR-CCM+ meshing utilities (see Figure A1 in Appendix A). The utilized meshes were tested and results were found to be grid independent (see Figure A2 in Appendix B).
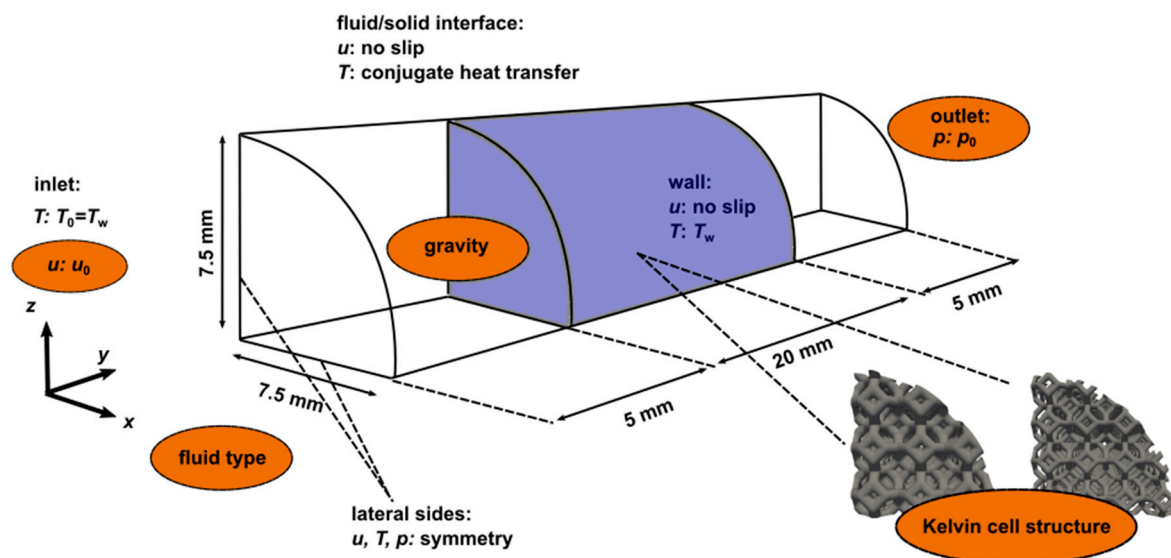

Figure 1. Illustration of model with boundary conditions. The orange highlighted fluid properties are investigated in this study.

Table 1. Properties of the investigated Kell cell lattices.

Parameter, Symbol.	Kelvin Cell 1 (KC1)	Kelvin Cell 2 (KC2)
open porosity, ε_O	0.724	0.845
specific surface area, S_V	1467.8 m^{-1}	1518.9 m^{-1}
cell diameter, d_c	1.924 mm	1.733 mm
strut diameter, d_s	0.591 mm	0.35 mm

The basic equations that are solved for a Newtonian fluid domain are the conservation of mass, momentum and energy:

$$\nabla \cdot (\rho_f \mathbf{U}) = 0, \tag{1}$$

$$\nabla \cdot (\rho_f \mathbf{U} \otimes \mathbf{U}) + \nabla \cdot \left(\mu \left(\nabla \otimes \mathbf{U} + (\nabla \otimes \mathbf{U})^T \right) - \frac{2}{3\mu} (\nabla \cdot \mathbf{U}) \mathbf{I} \right) - \nabla p + \rho_f \mathbf{g} = 0, \tag{2}$$

$$-\nabla \cdot (\rho_f \mathbf{U} h) - \nabla \cdot (\lambda_f \nabla T_f) = 0, \tag{3}$$

with ρ_f denoting the fluid's density, **U** the velocity field, h the enthalpy, μ the fluid's dynamic viscosity, T_f the fluid's temperature and λ_f the fluid's thermal conductivity. The solid phase is solely described by the conservation of energy

$$\lambda_s \left(\nabla^2 T_s \right) + S = 0, \tag{4}$$

with λ_s donating the solid thermal conductivity, T_s the solid temperature and S the specific artificial heat source. Furthermore, the fluid density is expressed via the ideal gas law.

The solid properties are kept constant, whereas the fluid properties such as dynamic viscosity, specific heat and thermal conductivity depend on the temperature (see Table 2). The model properties and assumptions are also listed in Table 2 and the basic boundary conditions can be found in Figure 1. In this study, fluid and wall temperatures are kept constant as a fixed temperature boundary at 500 K. This way, the only energy that enters the system is due to the volumetric heat source. Thermal radiation is not explicitly considered in the simulation as the temperatures are moderate and this study wants to investigate heat transport of fluid properties independently. Moreover, the influence of radiation has already been quantified in a comparable setup [15]. Furthermore, turbulence effects were taken into account through a *realizable k-ε* RANS turbulence model with *All y$^+$ wall-treatment* [34].

Table 2. Properties of this study's model.

Property		Assumption
Fluid dynamic viscosity	μ	Sutherland equation
Fluid heat capacity	$c_{p,f}$	polynomial
Fluid thermal conductivity	λ_f	Sutherland equation
Fluid density	δ_f	ideal gas law
Superficial velocity	v	const. (0.1–4 m s^{-1})
Pore Reynolds number (air)	$Re_p = \frac{v \cdot d_s \cdot \rho}{\mu}$	const. (0.3–76)
Wall/inlet temperature	$T_w = T_{in}$	const. (500 K)
Outlet pressure	p	const. (1–10 bar)
Solid heat capacity	$c_{p,s}$	const. (1000 J kg^{-1} K^{-1}).
Solid thermal conductivity	λ_s	const. (5 W m^{-1} K^{-1})
Solid density	δ_s	const. (3950 kg m^{-3})
Solid heat source	S	const. (total: 12.5 W)
Gravitational acceleration		considered
Turbulence		Realizable *k-ε* RANS (All *y$^+$* wall-treatment)
Radiation		neglected [15]

For studying the influence of gravitational acceleration in different directions, gravity is considered in y direction (in flow direction, representing a vertical reactor) as well as in z direction (perpendicular to flow, representing a horizontal reactor). Additionally, the varied and investigated properties are highlighted in orange in Figure 1.

In our previous studies, similar models were validated against pressure drop correlations, heat transfer correlations and verified against CFD data [15,19]. Here, the principal changed model property is the CAD-created geometry. We therefore omit the validation as the models are virtually identical.

3. Results and Discussion

All simulated cases have a total heat source of S = 12.5 W, which would correspond to a 50 W total heat source in a full foam setup (i.e., four quarters). As already described, the only thermal energy entering the system is due to the volumetric heat source (i.e., heat production in the solid foam). The global energy balance thus reads

$$S = 12.5\,\text{W} = Q_{SF} + Q_{SW}, \tag{5}$$

with Q_{SF} being the transferred heat flow from fluid to solid and Q_{SW} being the conducted heat flow from solid to the wall. Which heat removal mechanism dominates (i.e., convection or conduction), can be expressed through the specific heat flow from solid to wall $Q_{SW} \, S^{-1}$ through non-dimensionalization of Equation (4). For values above 0.5, thermal conduction is the dominant mechanism and for values below 0.5 convection is the dominant one. We note that due to the normalization by the heat source intensity, the actual implemented heat source value becomes less crucial. In our previous study it was shown that in the heat source intensity range between 5 W and 150 W temperature increases (in solid and fluid phases) and heat flows show the almost identical values.

The impact of the several investigated fluid properties on the heat flows is shown in Figure 2. Panel a shows the specific heat flow for a superficial velocity of the two investigated foams up to 4 m s^{-1}. Previous studies only investigated heat flows with coupled heat production in the solid has only up to 0.51 m s^{-1} [15,19]. Obviously, both foam structures switch from being dominated by conduction to being dominated by convection at a certain velocity. KC2 switches at a superficial velocity of approximately $v = 1.2 \text{ m s}^{-1}$ whereas KC1 switches not until a superficial velocity of approximately $v = 3 \text{ m s}^{-1}$. This is most certainly based on the different strut diameters of the foams (KC1: $d_s = 0.591$ mm compared to KC1: $d_s = 0.35$ mm), which ensures a better radial heat removal for KC1 through thermal conduction. This is line with the findings from the studies of Bracconi et al. [11] and Bianchi et al. [21], that investigated the role of the strut diameter in conductive heat transport.
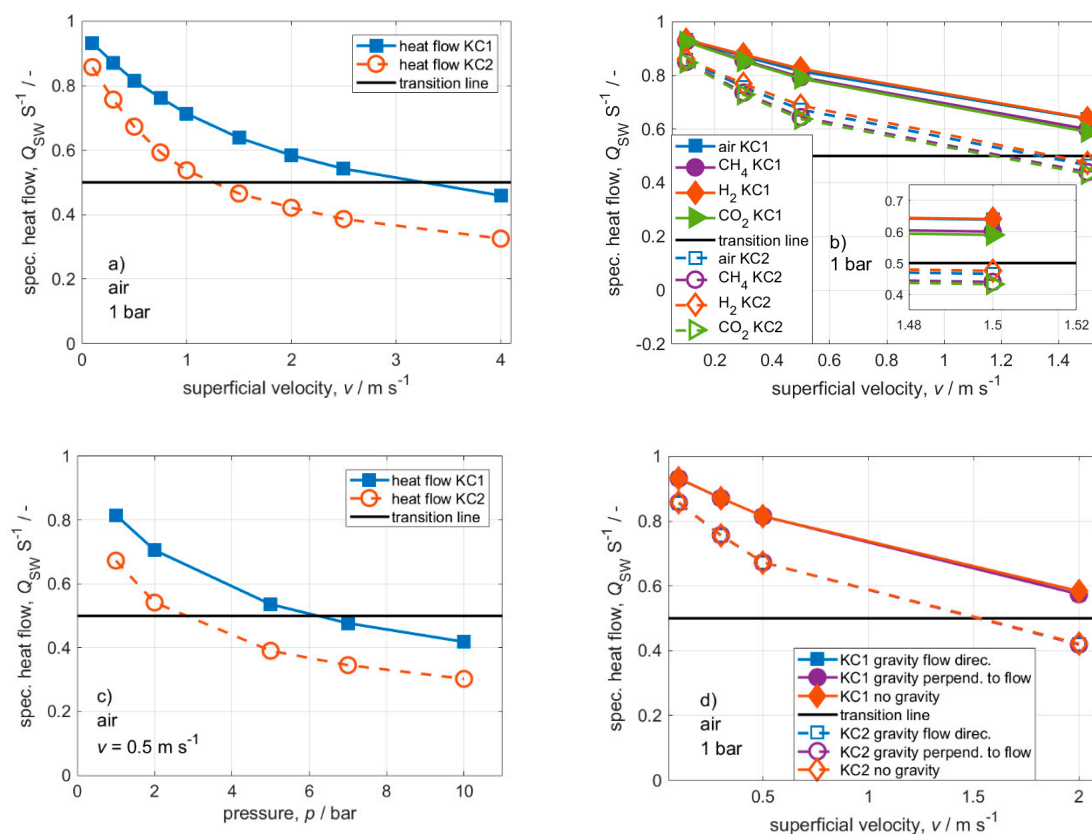

Figure 2. Heat flows for fluid property variation (**a**) Increase in inlet velocity incl. turbulence modelling; (**b**) Influence of fluid type; (**c**) Influence of pressure; (**d**) Influence of gravitational acceleration. Conditions: $S = 12.5$ W; $\lambda_s = 5 \text{ W m}^{-1} \text{ K}^{-1}$.

Figure 2a shows results using air as fluid as usually done in literature. Panel b shows the impact of the gas type, which is related to the CO_2 methanation, on heat removal. For both KC's, the difference in computed heat flows does not change distinctively, although a small difference between air and hydrogen on the one side and methane and carbon dioxide on the other side becomes

apparent. The small differences between the gas types can be explained through the interplay of gas viscosity, density, heat capacity and thermal conductivity which change over temperature for each gas individually. The order of thermal conductivities for the gases at 1 bar from highest to lowest is air, carbon dioxide, methane and hydrogen which is not the same order as in Panel b.

The influence of the pressure on the simulated heat flows at $v = 0.5$ m s^{-1} is shown in Figure 2c. Again, most of the literature investigated heat transport phenomena in foams only at 1 bar absolute pressure [14,35]. With increasing pressure, the heat transport switches from conduction dominated to convection dominated for both foams. At a pressure of 6 bar, both foams dominantly remove heat over convection and hence lose their advantage over standard pellets. The consideration of the actual working pressure thus influences the performance of the catalyst carriers tremendously. Structures that are designed to work efficiently, i.e., conduction dominated, at 1 bar, might already lose their efficiency at 2.5 bar (compare KC2 in panel c). The general effect is obvious, as both gas density and thus the ability of the fluid to cool down the foam via convection increase with pressure.

Often, CFD models omit gravitational acceleration [14,18,19]. Depending on the reactor setup (vertical pipe or horizontal pipe), gravitational acceleration affects the fluid in flow direction (vertical setup) or perpendicular to the flow direction (horizontal setup). Figure 2d shows the specific heat flow as a function of superficial velocity for both foams with gravity in flow direction, perpendicular to the flow as well as neglected gravity. In the investigated superficial velocity range (0.1–2 m s^{-1}), no significant influence of the consideration of gravity could be found. The reason probably lies in forced convection (i.e., pronounced velocity) being a lot more substantial for the overall convection than natural convection (i.e., effect of gravity). To our knowledge, correlations for the Grashof and Rayleigh numbers for this temperature distribution together with the velocity and pressure do not exist. Thus, this result could not have been anticipated by observing dimensionless numbers alone.

The analyzed heat flows for elevated velocities, changing fluid type, influence of pressure and gravity show the influence of the fluid properties on the overall heat transport in open-cell foam carriers. Additionally, Figure 3 shows the corresponding solid temperature rises of the cases shown in Figure 2. For brevity, we only show maximum temperature rises of the solid (instead of additional solid mean and fluid max/mean temperature rises) as they represent the entire solid temperature distribution in foams satisfactory [19]. In Figure 3, it can be seen that the curves of temperature rises of the two structures converge in the convection dominant regime. This behavior happens regardless of the applied pressure or superficial velocity (see panels a and c). Hence, at certain velocities (>3 m s^{-1}) and pressure (>7 bar), the temperature increase seems to be become independent of the foam geometry.
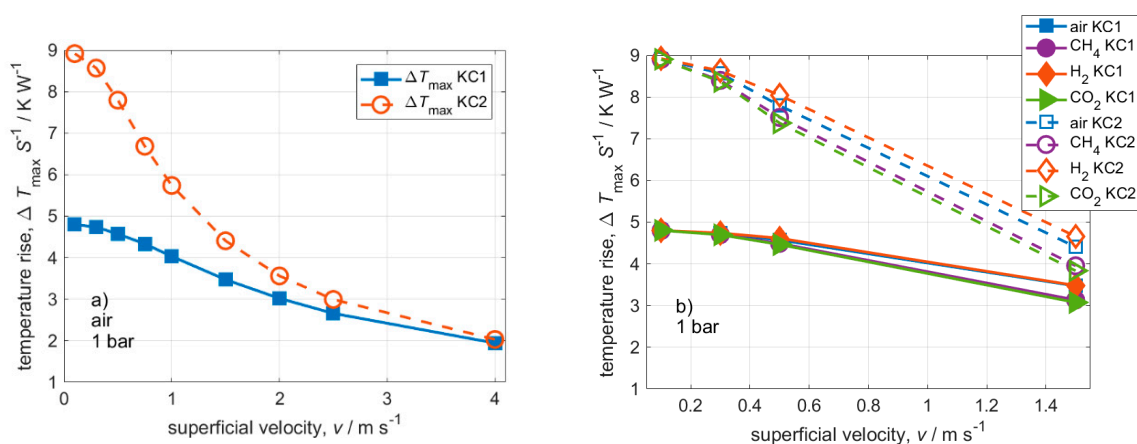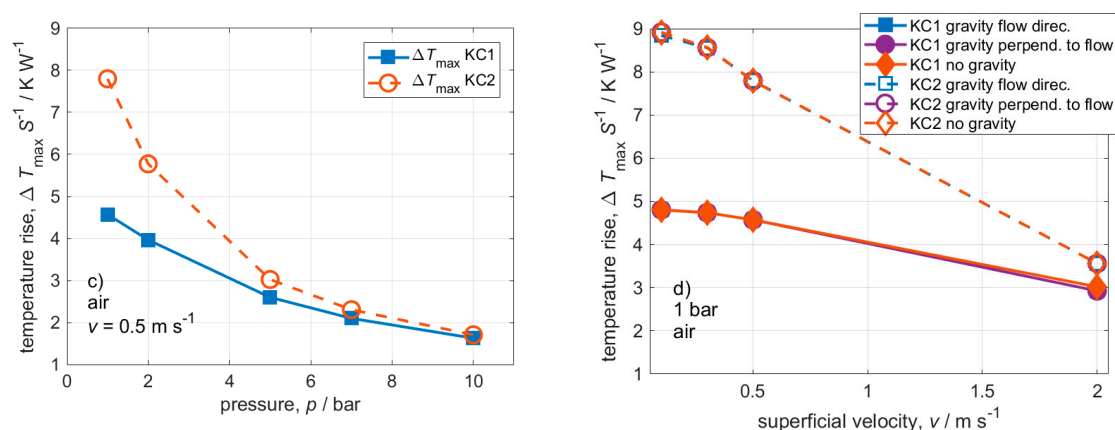

Figure 3. *Cont.*

Figure 3. Solid temperature rises per applied heat source intensity for fluid property variation (**a**) Increase in inlet velocity incl. turbulence modelling; (**b**) Influence of fluid type; (**c**) Influence of pressure; (**d**) Influence of gravitational acceleration. Conditions: $S = 12.5$ W; $\lambda_s = 5$ W m^{-1} K^{-1}.

For superficial velocities lower or equal than 1.5 m s^{-1}, the influence of the fluid type on the temperature rise varies for the two structures (see Figure 3b). The effect of the fluid type on the temperature rise increases with convective heat transport. Therefore, KC2 has a more pronounced difference (starting from 0.3 m s^{-1}) than KC1 (difference obvious starting from 1.5 m s^{-1}). This behavior could be expected as the fluid type influences the convective heat transport and becomes more important when the overall contribution of convection increases. To conclude, the fluid type seems to be less influential in the dominant conduction area where a structured foam reactor should be operated. Equivalently to the heat flows, no significant effect of gravity on the temperature rise could be found (Figure 3d).

4. Conclusions

This study analyzed the often-neglected influence of fluid properties on heat transport in open-cell foam reactors. As pointed out, usually heat transport in open-cell foams is investigated using air at 1 bar pressure absolute.

When foams are designed as catalyst carriers (for, e.g., dynamic CO_2 methanation), they should at best remove all heat radially via conduction (here: for working pressure between 4 and 10 bar, the velocity should be lower 0.5 m s^{-1}). At elevated velocities even structures with relatively thick struts can shift into the convection dominated regime. Not only for elevated velocities, but especially for pressure higher than 1 bar (usual operation conditions of CO_2 methanation 4–10 bar) the shift towards convection being dominant might proceed rapidly. In contrast, the choice of fluid mixture seems not as significant as pressure and velocity ranges. Obviously, this has to be checked for other gases of other reactions or inert gases. Nevertheless, air seems a reasonable fluid to study the general heat transport behavior of new foam designs, as the deviations of thermal fields to other gases are not that severe. This way, fluid mixture equations can be omitted and computational effort can be reduced. Additionally, the reactor orientation (represented through gravity) does not seem to have an impact on the heat transport in foams which is relevant for heterogeneous catalysis.

In conclusion, for the design of structured reactors for highly exothermic gas phase reactions, it is crucial to consider the exact velocity and pressure ranges of the investigated reaction. This is especially important, when the catalyst carriers are designed for dynamic or changing load operation. This type of operation might cause tremendous jumps in superficial velocity, pressure or fluid composition which further might influence the overall heat transport and might cause a thermal runaway or serious harm to the catalyst.

Nomenclature

Latin

c_p	isobaric heat capacity, J kg^{-1} K^{-1}
d_c	cell diameter, m
d_s	strut diameter, m
g	gravitational acceleration, 9.81 m s^{-2}
Q	heat flow, W
Q_{SF}	heat flow solid to fluid, W
Q_{SW}	heat flow solid to wall, W
h	specific enthalpy, J kg^{-1}
p	pressure, Pa
S	total heat source intensity, W
S_v	specific surface area, m^{-1}
T	temperature, K
T_w	wall temperature, K
T_{max}	maximum temperature, K
U	velocity, m s^{-1}
v	superficial velocity, m s^{-1}

Greek

ε_O	open porosity, -
μ	dynamic viscosity, Pa s
λ	thermal conductivity, W m^{-1} K^{-1}
ρ	density, kg m^{-3}

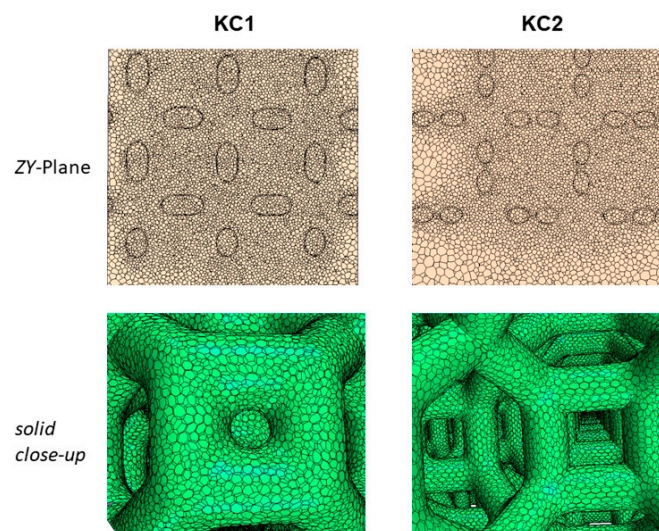## Appendix A. Depiction of Volume Meshes

Figure A1. Depiction of volume meshes that were used in this study.
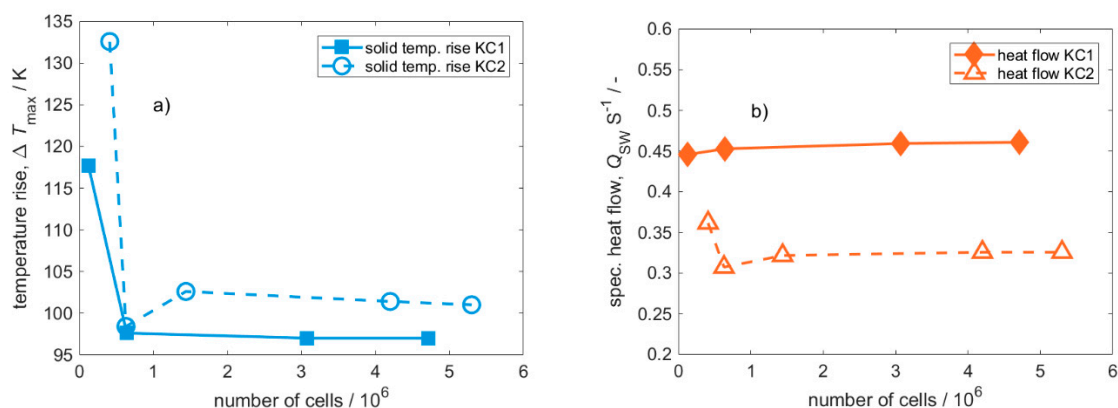
Appendix B. Grid Independence Study

Figure A2. Grid independence study. (**a**) Solid temperature rise from initial 500 K plotted against number of cells; (**b**) specific heat flow from solid to wall plotted against number of cells. For both used geometries, the second-largest meshes (KC1: 3.1 mio. Cells; KC2 4.1 mio cells) were found to give reasonable results. Conditions: air; p = 1 bar, v = 4 m s^{-1}.

References

1. Kiewidt, L.; Thöming, J. Multiscale modelling of monolithic sponges as catalyst carrier for the methanation of carbon dioxide. *Chem. Eng. Sci. X* **2019**, *2*, 100016. [CrossRef]
2. Stiegler, T.; Meltzer, K.; Tremel, A.; Baldauf, M.; Wasserscheid, P.; Albert, J. Development of a Structured Reactor System for CO_2 Methanation under Dynamic Operating Conditions. *Energy Technol.* **2019**, *7*, 1900047. [CrossRef]
3. Gräf, I.; Ladenburger, G.; Kraushaar-Czarnetzki, B. Heat transport in catalytic sponge packings in the presence of an exothermal reaction: Characterization by 2D modeling of experiments. *Chem. Eng. J.* **2016**, *287*, 425–435. [CrossRef]
4. Vogt, C.; Monai, M.; Kramer, G.J.; Weckhuysen, B.M. The renaissance of the Sabatier reaction and its applications on Earth and in space. *Nat. Catal.* **2019**, *2*, 188–197. [CrossRef]
5. Kalz, K.F.; Kraehnert, R.; Dvoyashkin, M.; Dittmeyer, R.; Gläser, R.; Krewer, U.; Reuter, K.; Grunwaldt, J.D. Future Challenges in Heterogeneous Catalysis: Understanding Catalysts under Dynamic Reaction Conditions. *ChemCatChem* **2017**, *9*, 17–29. [CrossRef]
6. Rönsch, S.; Schneider, J.; Matthischke, S.; Schlüter, M.; Götz, M.; Lefebvre, J.; Prabhakaran, P.; Bajohr, S. Review on methanation—From fundamentals to current projects. *Fuel* **2016**, *166*, 276–296. [CrossRef]
7. Kiewidt, L.; Thöming, J. Predicting optimal temperature profiles in single-stage fixed-bed reactors for CO2-methanation. *Chem. Eng. Sci.* **2015**, *132*, 59–71. [CrossRef]
8. Kiewidt, L.; Thöming, J. Pareto-optimal design and assessment of monolithic sponges as catalyst carriers for exothermic reactions. *Chem. Eng. J.* **2019**, *359*, 496–504. [CrossRef]
9. Gräf, I.; Rühl, A.K.; Kraushaar-Czarnetzki, B. Experimental study of heat transport in catalytic sponge packings by monitoring spatial temperature profiles in a cooled-wall reactor. *Chem. Eng. J.* **2014**, *244*, 234–242. [CrossRef]
10. Dixon, A.G.; Partopour, B. Computational Fluid Dynamics for Fixed Bed Reactor Design. *Annu. Rev. Chem. Biomol. Eng.* **2020**, *11*, 109–130. [CrossRef] [PubMed]
11. Bracconi, M.; Ambrosetti, M.; Maestri, M.; Groppi, G.; Tronconi, E. A fundamental analysis of the influence of the geometrical properties on the effective thermal conductivity of open-cell foams. *Chem. Eng. Process. Process Intensif.* **2018**, *129*, 181–189. [CrossRef]
12. Ranut, P.; Nobile, E.; Mancini, L. High resolution X-ray microtomography-based CFD simulation for the characterization of flow permeability and effective thermal conductivity of aluminum metal foams. *Exp. Therm. Fluid Sci.* **2015**, *67*, 30–36. [CrossRef]
13. Iasiello, M.; Bianco, N.; Chiu, W.K.S.; Naso, V. Anisotropic convective heat transfer in open-cell metal foams: Assessment and correlations. *Int. J. Heat Mass Transf.* **2020**, *154*, 119682. [CrossRef]

14. Della Torre, A.; Montenegro, G.; Onorati, A.; Tabor, G. CFD characterization of pressure drop and heat transfer inside porous substrates. *Energy Procedia* **2015**, *81*, 836–845. [CrossRef]

15. Sinn, C.; Kranz, F.; Wentrup, J.; Thöming, J.; Wehinger, G.D.; Pesch, G.R. CFD Simulations of Radiative Heat Transport in Open-Cell Foam Catalytic Reactors. *Catalysts* **2020**, *10*, 716. [CrossRef]

16. Zafari, M.; Panjepour, M.; Emami, M.D.; Meratian, M. Microtomography-based numerical simulation of fluid flow and heat transfer in open cell metal foams. *Appl. Therm. Eng.* **2015**, *80*, 347–354. [CrossRef]

17. Wu, Z.; Caliot, C.; Flamant, G.; Wang, Z. Numerical simulation of convective heat transfer between air flow and ceramic foams to optimise volumetric solar air receiver performances. *Int. J. Heat Mass Transf.* **2011**, *54*, 1527–1537. [CrossRef]

18. Razza, S.; Heidig, T.; Bianchi, E.; Groppi, G.; Schwieger, W.; Tronconi, E.; Freund, H. Heat transfer performance of structured catalytic reactors packed with metal foam supports: Influence of wall coupling. *Catal. Today* **2016**, *273*, 187–195. [CrossRef]

19. Sinn, C.; Pesch, G.R.; Thöming, J.; Kiewidt, L. Coupled conjugate heat transfer and heat production in open-cell ceramic foams investigated using CFD. *Int. J. Heat Mass Transf.* **2019**, *139*, 600–612. [CrossRef]

20. Ambrosio, G.; Bianco, N.; Chiu, W.K.S.; Iasiello, M.; Naso, V.; Oliviero, M. The effect of open-cell metal foams strut shape on convection heat transfer and pressure drop. *Appl. Therm. Eng.* **2016**, *103*, 333–343. [CrossRef]

21. Bianchi, E.; Schwieger, W.; Freund, H. Assessment of Periodic Open Cellular Structures for Enhanced Heat Conduction in Catalytic Fixed-Bed Reactors. *Adv. Eng. Mater.* **2016**, *18*, 608–614. [CrossRef]

22. Diani, A.; Bodla, K.K.; Rossetto, L.; Garimella, S.V. Numerical investigation of pressure drop and heat transfer through reconstructed metal foams and comparison against experiments. *Int. J. Heat Mass Transf.* **2015**, *88*, 508–515. [CrossRef]

23. Du, S.; Tong, Z.X.; Zhang, H.H.; He, Y.L. Tomography-based determination of Nusselt number correlation for the porous volumetric solar receiver with different geometrical parameters. *Renew. Energy* **2019**, *135*, 711–718. [CrossRef]

24. Aguirre, A.; Chandra, V.; Peters, E.A.J.F.; Kuipers, J.A.M.; Neira D'Angelo, M.F. Open-cell foams as catalysts support: A systematic analysis of the mass transfer limitations. *Chem. Eng. J.* **2020**, *393*, 124656. [CrossRef]

25. Dong, Y.; Korup, O.; Gerdts, J.; Roldán Cuenya, B.; Horn, R. Microtomography-based CFD modeling of a fixed-bed reactor with an open-cell foam monolith and experimental verification by reactor profile measurements. *Chem. Eng. J.* **2018**, *353*, 176–188. [CrossRef]

26. Della Torre, A.; Lucci, F.; Montenegro, G.; Onorati, A.; Dimopoulos Eggenschwiler, P.; Tronconi, E.; Groppi, G. CFD modeling of catalytic reactions in open-cell foam substrates. *Comput. Chem. Eng.* **2016**, *92*, 55–63. [CrossRef]

27. Wehinger, G.D.; Heitmann, H.; Kraume, M. An artificial structure modeler for 3D CFD simulations of catalytic foams. *Chem. Eng. J.* **2016**, *284*, 543–556. [CrossRef]

28. Bracconi, M.; Ambrosetti, M.; Maestri, M.; Groppi, G.; Tronconi, E. A fundamental investigation of gas/solid mass transfer in open-cell foams using a combined experimental and CFD approach. *Chem. Eng. J.* **2018**, *352*, 558–571. [CrossRef]

29. Frey, M.; Bengaouer, A.; Geffraye, G.; Edouard, D.; Roger, A.C. Aluminum Open Cell Foams as Efficient Supports for Carbon Dioxide Methanation Catalysts: Pilot-Scale Reaction Results. *Energy Technol.* **2017**, *5*, 2078–2085. [CrossRef]

30. Montenegro Camacho, Y.S.; Bensaid, S.; Lorentzou, S.; Vlachos, N.; Pantoleontos, G.; Konstandopoulos, A.; Luneau, M.; Meunier, F.C.; Guilhaume, N.; Schuurman, Y.; et al. Development of a robust and efficient biogas processor for hydrogen production. Part 2: Experimental campaign. *Int. J. Hydrogen Energy* **2018**, *43*, 161–177. [CrossRef]

31. Bianchi, E.; Groppi, G.; Schwieger, W.; Tronconi, E.; Freund, H. Numerical simulation of heat transfer in the near-wall region of tubular reactors packed with metal open-cell foams. *Chem. Eng. J.* **2015**, *264*, 268–279. [CrossRef]

32. Nie, Z.; Lin, Y.; Tong, Q. Modeling structures of open cell foams. *Comput. Mater. Sci.* **2017**, *131*, 160–169. [CrossRef]

33. STAR-CCM+. Available online: https://www.plm.automation.siemens.com/global/en/products/simcenter/STAR-CCM.html (accessed on 6 October 2020).

34.　Wehinger, G.D. Radiation Matters in Fixed-Bed CFD Simulations. *Chemie-Ingenieur-Technik* **2019**, *91*, 583–591. [CrossRef]

35.　Iasiello, M.; Cunsolo, S.; Bianco, N.; Chiu, W.K.S.; Naso, V. Developing thermal flow in open-cell foams. *Int. J. Therm. Sci.* **2017**, *111*, 129–137. [CrossRef]

Publisher's Note: MDPI stays neutral with regard to jurisdictional claims in published maps and institutional affiliations.